Theor Chim Acta (1992) 82: 321–337

Theoretica Chimica Acta

Analysis of the transition from normal modes to local modes in a system of two harmonically coupled Morse oscillators

Giovanna Longhi[1], Sergio Abbate[1], Claudio Zagano[2], Giovanni Botto[3], and Laure Ricard-Lespade[4]

[1] Dipartimento di Chimica Fisica, Università di Palermo, via Archirafi 26, I-90123 Palermo, Italy

[2] via Carlo Porta 16, I-20067 Paullo, Milano, Italy

[3] via Astura 6, I-20141 Milano, Italy

[4] Laboratoire de Spectroscopie Moleculaire et Cristalline, C.N.R.S., Université de Bordeaux I, 351 Crs. de la Liberation, F-33405 Talence Cedex, France

Received December 6, 1990/Accepted August 13, 1991

Summary. The system consisting of two Morse oscillators coupled via either a potential or a kinetic quadratic term is considered. The corresponding classical equations of motion have been numerically integrated and the initial conditions have been systematically analyzed in the regime of low total excitation energy of the system. Particular attention was paid to the full characterization of an intermediate type of motion, herein called transition mode, which appears at total energy values in between those typical of normal modes and those where local and normal modes coexist. A previously proposed perturbative approach (Jaffé C, Brumer P (1980) J Chem Phys 73:5646) is reanalyzed and compared with the results of numerical experiments, with the purpose of lending further support to the existence of transition modes.

Key words: Anharmonic oscillators – Local modes – Classical dynamics – Poincaré surfaces of section

1. Introduction

The local mode model was first proposed in order to provide a simple explanation of the remarkably simple spectra in the high overtone region of organic molecules containing XH bonds (X = C, O, N, . . .) [1]. The subsequent development of the thermal lensing [2] and photoacoustic techniques [3] has allowed one to test this model more precisely; Raman spectroscopy [4] and near infrared circular dichroism [5] have also been employed for this purpose.

The theoretical justification of the local mode behavior came later. For example, for systems with 2, 3, or 4 equivalent BA bond stretchings, described as Morse oscillators and harmonically coupled, Mills and Robiette [6] proved that the local mode behavior takes place at about the second overtone ($v = 3$). This result is obtained by a quantum perturbative treatment starting either from a normal mode basis set or a local mode basis set. The equivalence of the two approaches was first demonstrated in a letter by Lehman [7a]. A nice generalization of this theory is given in [7b, 8, 9]. In parallel, the classical equations of

motion for an ABA molecule (without the bending motion) were reconsidered, both numerically and analytically, in order to characterize the types of molecular motions taking place under the influence of nonlinear forces [10–13]. The above authors considered the behavior of various observables in their numerical experiments, namely they have presented diagrams in configuration space (Lissajous maps) [10, 11], diagrams in phase space such as the Poincaré surfaces of section [10, 12], and finally the time dependence of individual oscillators energies [13]. In both [12] and [13] the results of the numerical experiments were compared with an analytical approach consisting in the development of the interaction potential of the two bonds as a Fourier series, whose individual terms depended upon actions and angles of the isolated Morse oscillators. Recently Li et al. [14] have made use of bifurcation theory to characterize the fixed points of the Hamiltonian of two coupled anharmonic oscillators, and have described the normal to local transition with respect to coupling strength and dissymmetry of the two bonds.

Further developments of the theory comprised the study of anharmonic stretching modes interacting with bendings and rotations. In particular, the consideration of Fermi resonance among YXH bending and XH stretching [15, 16] has allowed one to explain satisfactorily the behavior of bandwidths in the progression of benzene overtones up to $\Delta v = 10$ [15, 17], and also to define the nature of extra bands at a specific overtone order in haloforms [16]. Furthermore, the rotational structure of overtone bands was also studied both theoretically and experimentally [18–21]. The importance of these studies for fast kinetics was pointed out in all the above papers and has been recently reviewed by Hutchinson [22].

In this work we go back to the classical dynamics of the simple ABA system, with the purpose of studying more closely the transition region between normal modes and local modes. In Sect. 2 we will present some numerical experiments, where we varied systematically all possible initial conditions, and analyzed the results in terms of most of the various kinds of diagrams described above. In Sect. 3 we will interpret the new results obtained in Sect. 2 using the model developed by Jaffé and Brumer [12], who analyzed the coupling term as a function of local mode properties. By these two approaches, i.e., numerical calculations and perturbative treatment, we have characterized a new kind of modes which have an intermediate behavior between normal and local modes and which we have called "transition modes". They appear at energies lower than local mode threshold and coexist with local and normal modes.

2. Numerical experiments

As we have already mentioned in the introduction, the purpose of this paper is the characterization of vibrational modes for two linearly coupled anharmonic oscillators in the relatively low energy region, far from dissociation. We have achieved this by numerical integration of the classical equations of motion derived from the Hamiltonian:

$$H = \sum_{i=1}^{2} \left\{ \frac{p_i^2}{2m} + D_i[1 - \exp(l_i - l_{i0})]^2 \right\} + K(l_1 - l_{10})(l_2 - l_{20}) \tag{1}$$

Here l_i are the instantaneous bond lengths, whose equilibrium values are l_{i0}; p_i are their conjugated momenta; m is the reduced mass for both bonds. We define the parameters for the Morse potential D_i and a_i in terms of the mechanical

wavenumber ω_i^h and anharmonicity constants χ_i (cm^{-1}) [11]:

$$D_i = \frac{hc\omega_i^{h2}}{4\chi_i} \tag{2}$$

$$a_i = \sqrt{\frac{8\pi^2 mc\chi_i}{h}} \tag{3}$$

(h = Planck's constant, c = speed of light). Even though our purpose is not a detailed comparison with experiment, we chose values close to those for aliphatic CH's, namely $\omega_1^h = \omega_2^h = 3000\ cm^{-1}$ and $\chi_1 = \chi_2 = 60\ cm^{-1}$, $m = 1$ a.m.u., $l_{10} = l_{20} = 1.0$ Å.

We have considered different values, both positive and negative, for the interaction force constant K and show results for $K = \pm 0.1$ mdyne/Å, neglecting at first any kinetic coupling. The equations of motion were integrated by means of a 4th-order Runge–Kutta algorithm with a stepsize of 0.01 femtosec and total integration times of up to 4 picosec. The numerical results thus obtained were examined with the aid of different plots:

(a) time evolution of individual oscillator energies, defined as:

$$E_i(t) = p_i^2/2m + D_i(1 - \exp(-a_i(l_i - l_{i0})))^2$$

(b) time evolution of stretching coordinates $l_i(t)$

(c) Poincaré surfaces of section (PSS), namely plots of the values $\Delta l_2(t) = l_2(t) - l_{20}$ and $p_2(t)$ at all times t for which $\Delta l_1 = 0, p_1 > 0$

(d) plots of the period T of $E_i(t)$ vs. the maximum energy difference ΔE_{max} between the two oscillators achieved during time evolution.

In order to be able to discuss the problem of the title of the present paper, let us first consider the definition of normal modes and local modes, in the presence of anharmonicity and at different values of total energy $E_T = E_1(0) + E_2(0)$.

(a) Normal modes: It has been pointed out that, when one plots individual bond energies vs. time, one sees that energy is exchanged between the two oscillators during a period T in such a way that the bond energies' averages over long times are equal: $\langle E_1(t)\rangle = \langle E_2(t)\rangle$, as illustrated in Fig. 1A [13]. Another characteristic of normal modes is "phase locking" of the two oscillators. We remark that a requisite similar to this has been assumed in numerous textbooks as the most characteristic of normal modes, namely a fixed phase relation between oscillators [23]. Indeed, for the Hamiltonian studied here, if one plots the bonds' lengths $l_1(t)$ and $l_2(t)$ vs. time one finds that they vary periodically with a double periodicity: a short period in the range of femtoseconds that corresponds to the oscillations of the individual bonds and a longer one, that we have called T, in the range of 100 to 1000 femtosec that corresponds to amplitude (and energy) modulation of bond oscillations. Such a modulation is originated by the fact that the two CH oscillators, due to anharmonicity, possess slightly different frequencies. In the case of normal modes one can notice from Fig. 1A that $l_1(t)$ and $l_2(t)$ always differ by less than a short period, that is to say their average frequency over long times is the same $\langle\omega_1(t)\rangle = \langle\omega_2(t)\rangle$ (in fact normal modes can be described as originated by a nonlinear resonance between two local oscillators [12]).

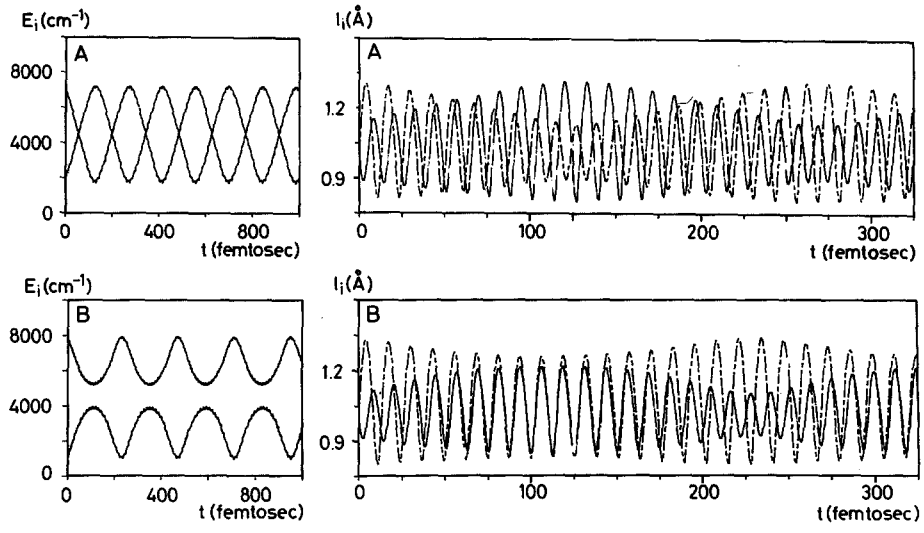

Fig. 1A,B. Oscillators energies and lengths vs. time for normal modes (**A**) and local modes (**B**). Total energy $E_T = 9000\ \text{cm}^{-1}$, $K = -0.1$ mdyne/Å; (**A**) $\Delta E_{in} = 5500\ \text{cm}^{-1}$, A; (**B**) $\Delta E_{in} = 6600$ cm, A

(b) Local modes: These modes are characterized by the fact that one oscillator has always a higher energy than the other [13], and that there is no "phase locking" between $l_1(t)$ and $l_2(t)$ (Fig. 1B): oscillator number 2, at lower energy, gains a whole short period of oscillation with respect to oscillator number 1 in every long period T. A consequence of this is that the averages of the oscillators frequencies over times greater than T are as follows: $\langle \omega_1(t) \rangle > \langle \omega_2(t) \rangle$. In conclusion one can say that the nonlinear effect leading to energy modulation is still present, whereas the nonlinear resonance between the two oscillators is not.

2.1. Varying values of the total energy E_T

In order to characterize the normal mode–local mode transition we carried out numerical experiments at different total energies from $E_T = 500\ \text{cm}^{-1}$ up to $E_T = 15{,}000\ \text{cm}^{-1}$ (far from dissociation and chaotic regimes). A meaningful choice of the PSS obtained for the cases $K = \pm 0.1$ mdyne/Å is proposed in Fig. 2. Different trajectories in the PSS correspond to different initial conditions. In particular we varied $\Delta E_{in} = E_1(0) - E_2(0)$ while taking the two oscillators at their potential minimum at time $t = 0$, moving either in the same direction (S) or in opposite directions (A). Alternatively one can set $\Delta E_{in} = 0$ and vary the initial position of one of the two oscillators with respect to the equilibrium position; it can be shown that similar trajectories are obtained. Figure 2 shows the three kinds of PSS that we found, which contain, to a different extent, the different kinds of modes.

(**a**) At low energies ($E_T < 1500\ \text{cm}^{-1}$, Fig. 2A, 2D), there are two families of curves surrounding two stable fixed points, one family generated from initial conditions (S), the other one from initial conditions (A). The two stable points have phase space coordinates $p_2 > 0$, $\Delta l_2 = 0$ and $p_2 < 0$, $\Delta l_2 > 0$, respectively. They correspond to the purely symmetric normal mode and to the almost pure

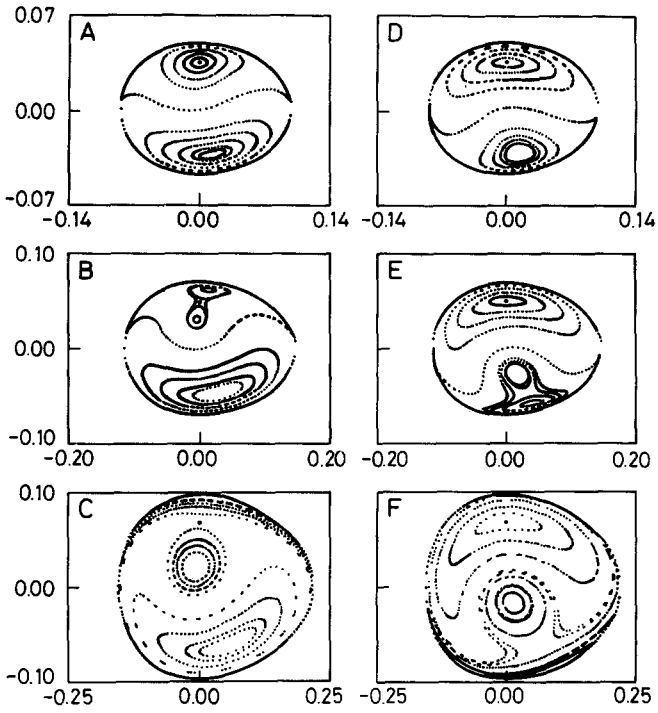

Fig. 2A–F. Poincaré surfaces of section for two coupled Morse oscillators at three different values of the total energy E_T; (**A–C**) $K = -0.1$ mdyne/Å; (**D–F**) $K = +0.1$ mdyne/Å. Both oscillators start from the vibrational equilibrium. Ordinate axes are p_2 (units: a.m.u. A femtosec^{-1}). Abscissas are l_2 (units: Å). **A** $E_T = 1000\ \text{cm}^{-1}$. *lower half (lh):* antisymmetric normal modes. *higher half (hh):* symmetric normal modes. In both cases the curves are ordered from inside with $\Delta E_{in} = 0, 200, 400, 600, 800\ \text{cm}^{-1}$. Separating curve: $\Delta E_{in} = 1000\ \text{cm}^{-1}$. **B** $E_T = 2000\ \text{cm}^{-1}$. *lh:* antisymmetric normal modes, from inside: $E_{in} = 0, 400, 800, 1200, 1600\ \text{cm}^{-1}$. *hh:* symmetric normal modes and transition modes. *Central dot:* $\Delta E_{in} = 0\ \text{cm}^{-1}$, symmetric normal mode. *Inner couples of circles:* $\Delta E_{in} = \pm 800, \pm 1200\ \text{cm}^{-1}$, transition modes. *Bilobed curve:* $\Delta E_{in} = 1600\ \text{cm}^{-1}$, symmetric normal mode. *Separating curve:* $\Delta E_{in} = 2000\ \text{cm}^{-1}$. **C** $E_T = 4000\ \text{cm}^{-1}$. *lh:* antisymmetric normal modes, from inside: $\Delta E_{in} = 0, 1000, 2000, 3000\ \text{cm}^{-1}$. *hh:* symmetric normal modes, transition modes and local modes. *Central dot:* $\Delta E_{in} = 0$, symmetric normal mode. *Inner curves*, from inside: $\Delta E_{in} = \pm 3000, \pm 4000\ \text{cm}^{-1}$, *S* (transition modes), $\pm 2000, \pm 1000\ \text{cm}^{-1}$, *S* (local modes). **D** $E_T = 1000\ \text{cm}^{-1}$. *lh:* antisymmetric normal modes. *hh:* symmetric normal modes. Ordering as in A). **E** $E_T = 2000\ \text{cm}^{-1}$. *lh:* antisymmetric normal modes and transition modes. *External bilobed curves:* normal modes for $\Delta E_{in} = 0$ and $400\ \text{cm}^{-1}$ coincident, $800\ \text{cm}^{-1}$. *Inner couples of circles:* transition modes, for $\Delta E_{in} = \pm 1600, \pm 1200\ \text{cm}^{-1}$. *hh:* symmetric normal modes, $\Delta E_{in} = 0$, 400, 800, 1200, $1600\ \text{cm}^{-1}$ (from inside). **F** $E_T = 4000\ \text{cm}^{-1}$. *hh:* symmetric normal modes from $\Delta E_{in} = 0$, 1000, 2000, $3000\ \text{cm}^{-1}$, *S*, and 0, $1000\ \text{cm}^{-1}$, *A*. *hh: Inner curves*, from inside: $\Delta E_{in} = \pm 3500$ and $\pm 4000\ \text{cm}^{-1}$, *A* (transition modes), $\Delta E_{in} = \pm 3000$ and $\pm 2000\ \text{cm}^{-1}$, *A* (local modes)

antisymmetric normal mode respectively, since the sign of p_2 is the same or opposite to that of p_1. The PSS obtained with $\Delta E_{in} = E_T$ surrounds the family of curves of symmetric-type ($K < 0$) or antisymmetric-type ($K > 0$) normal modes and forms a separatrix between the two families. All modes are normal modes and have the characteristics illustrated above. At these values for E_T, both the symmetric and antisymmetric normal modes are stable, independently of the sign of K. Moreover one can notice that in both cases A and D of Fig. 2 ($K < 0$ and

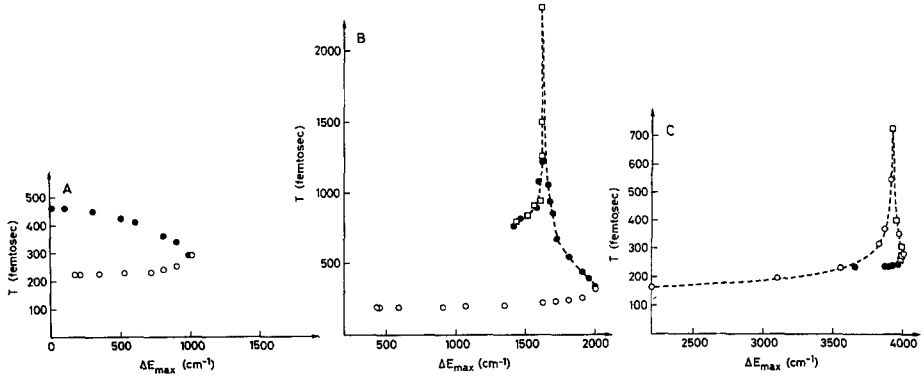

Fig. 3A–C. Plots of the period of energy exchange, T, vs. the maximum energy difference, $\Delta E_{\max}$. $K = -0.1$ mdyne/Å. **A** $E_T = 1000\ \mathrm{cm}^{-1}$; ●: initial symmetric excitation S; ○: initial antisymmetric excitation A. **B** $E_T = 2000\ \mathrm{cm}^{-1}$; ○: A; ●: S (in order of increasing initial energy difference ΔE_{in}); □: S (in order of decreasing ΔE_{in}). **C** $E_T = 4000\ \mathrm{cm}^{-1}$; ●: A; ○: S (in order of increasing ΔE_{in}); □: S (in order of decreasing ΔE_{in})

$K > 0$) there exists a "purely symmetric" motion that persists for an infinitely long time and is represented by the point in the PSS. In a paper written in 1961, Thiele and Wilson [24] pointed out, from basic mathematical properties, that two coupled anharmonic oscillators do admit a "purely symmetric" solution but not a purely antisymmetric one. We report in Fig. 3A the plot of the period T of energy exchange and phase locking vs. $\Delta E_{\max}$ for $K < 0$. There are two monotonic branches corresponding to symmetric and antisymmetric normal modes.

Before describing the next two regimes, we point out that in the literature only one of them is considered at higher E_T. Its PSS appear as presented in Fig. 2C and 2F. For $K < 0$, the symmetric mode is unstable, namely it is represented by a saddle point in the PSS, whereas the antisymmetric mode contains a center and is surrounded by normal mode trajectories. (The system for $K > 0$ behaves in a parallel way but here the "purely symmetric" mode is stable and there is a saddle point in the region of antisymmetric modes.) The circular shaped curves near the center ($\Delta l_2 = 0, p_2 = 0$) correspond to local modes of bond number 1, and the circular shaped curves near the maximum external circle correspond to local modes of bond number 2.

(b) At intermediate energies ($\approx 1750\ \mathrm{cm}^{-1} < E_T \leqslant 3151\ \mathrm{cm}^{-1}$ for $K = -0.1$ mdyne/Å and $\approx 1750\ \mathrm{cm}^{-1} < E_T \leqslant 2849\ \mathrm{cm}^{-1}$ for $K = 0.1$ mdyne/Å) there is a new situation where the local modes are not present yet. The curve for $\Delta E_{in} = E_T$ is still separatrix between symmetric-type modes and antisymmetric ones (Fig. 2B and 2E). However, for $K < 0$ the purely symmetric mode (and for $K > 0$ the antisymmetric one) becomes unstable. There are two new families of curves corresponding to positive ΔE_{in} and negative ΔE_{in}, and close to the symmetric fixed point $K < 0$ and to the antisymmetric fixed point for $K > 0$ but not surrounding it. These curves are the PSS of a new kind of modes, which we call *transition modes*. These modes are local from the point of view of energies since the two oscillators have different mean energies; normal from the point of view of phase relation since the two oscillators are phase locked (see Fig. 4).

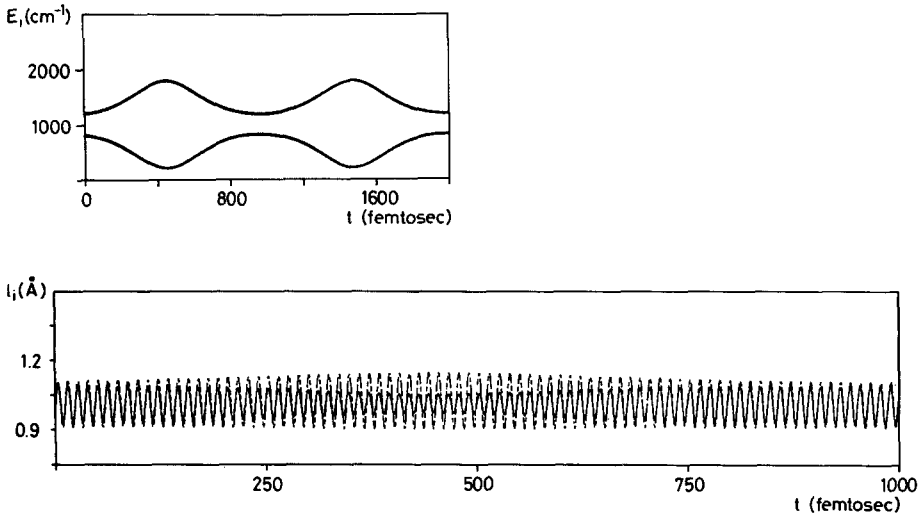

Fig. 4. Oscillators' energies and lengths vs. time for transition modes. Total energy $E_T = 2000\,\mathrm{cm}^{-1}$, $K = -0.1$ mdyne/A. Initial conditions: $\Delta E_{in} = 400$ cm, both oscillators at equilibrium, S

Previously, Child and Halonen [11] and Lawton and Child [25] hinted the existence of some kind of "transitional" modes, but did not elaborate too much on the idea. Thus a comparison with that found here is not possible. PSS curves (of Fig. 2B) containing both the symmetric point and the transition curves (for $K < 0$) are of normal type. In Fig. 3B, T is plotted vs. $\Delta E_{\max}$ for a case in this total energy region, with $K < 0$. It comprises three branches. The first one is obtained from initial conditions (A), it presents a monotonic behavior as in the lower energies case and corresponds to antisymmetric normal modes. Instead, with initial conditions (S), T vs. $\Delta E_{\max}$ shows a cusp. The left branch corresponds to the transition modes, the right branch to the normal modes. The cusp is at the purely symmetric point. It is noted that transition modes are obtained at low ΔE_{in} (and low $\Delta E_{\max}$) and normal modes at high $\Delta E_{\max}$. Finally, we observe that for a transition mode the larger $\Delta E_{\max}$ is, the greater the radius of the corresponding PSS curve is. Instead ΔE_{in} is not directly correlated with the data of the PSS (see caption of Fig. 3).

(c) The final regime of local modes plus normal modes is obtained for $K = -0.1$ mdyne/Å at $E_T > 3152\,\mathrm{cm}^{-1}$, and for $K = 0.1$ mdyne/Å at $E_T > 2850\,\mathrm{cm}^{-1}$ (Figs. 2C and 2F, respectively). The curve relative to $\Delta E_{in} = E_T$ is no more the separatrix between the families of curves corresponding to initial conditions (S) and (A); it is now similar to a circle and belongs to the family of curves classified as local in the literature. The "circles" outside the curve corresponding to $\Delta E_{in} = E_T$ are local modes and are obtained from both initial conditions (A) and (S). At relatively low total energies, there are also "circles" inside that curve. The latter correspond to persisting transition modes and are generated only from initial condition (S) or close to (S). These modes disappear with increasing E_T. For $K < 0$ no normal mode can be generated from initial conditions (S) except the purely symmetric one at $\Delta E_{in} = 0$. In Fig. 3C we report T vs. $\Delta E_{\max}$. We do not have anymore two curves for the two types of initial

conditions (S) and (A); regardless of the initial positions $l_1(0)$, $l_2(0)$ and momenta $p_1(0), p_2(0)$ all points T vs. $\Delta E_{\max}$ fall on a single cusp type curve which resembles the plot of the period of a pendulum vs. its energy [13, 26, 27]. When $K < 0$, the normal modes are on the left side of the cusp corresponding to the librational motions of the pendulum, and can be attained only by initial conditions of the type (A) for $\Delta E_{in} \neq 0$ and for the various initial phase differences with $\Delta E_{in} = 0$. The local modes are on the rotational side of this pendulum-type curve and can be generated by both initial conditions (A) and (S). The cusp-type behavior for T was first predicted theoretically by Sibert et al. [13] from basic considerations on the pendulum (see also [12, 25, and 27]). Here we just found "experimental" evidence for that anticipation. The cusp-type curve represents well only local and normal modes, whereas the residual transition modes correspond to the short almost constant branch.

2.2. *Study of another form of coupling*

We finally carried out numerical calculations on a system of two CH oscillators with both potential and kinetic coupling, namely we added to the Hamiltonian of Eq. (1) the term:

$$G_{12} p_1 p_2 \quad \text{with } G_{12} = (1/m_C) \cos\theta \tag{4}$$

Since the purpose of this part is to study some physically realistic model for CH_2, one can take θ as tetrahedral angle, m_C as the mass of the carbon atom and K as $+0.1$ mdyne/Å according to that found on most empirical force fields on n-paraffines [23, 28]. In Fig. 5 we merely present three PSS at different value of total energy E_T, each for every one of the three regimes described before. In this case, K and G_{12} have opposite sign and thus tend to cancel the effect of one another. Thus the first regime, where only normal modes are present, survives only for very low values of total energy; at $700\,\text{cm}^{-1}$ we already have the presence of transition modes. The point that gets unstable, giving rise to the transition modes and then local modes around $1000\,\text{cm}^{-1}$ is the symmetric one, as if there were an effective constant K_{eff} with negative sign.

In conclusion we found that the normal modes to local modes transition, as total energy increases, comes with the presence of transition modes, where the two oscillators are phase locked but have different mean energies. To further characterize all types of modes that we have commented on, we finally observe that:

(a) the same normal mode trajectory can be obtained either from a value ΔE_{in} or from the opposite value $-\Delta E_{in}$. In contrast, when for a given value for ΔE_{in}, a local mode trajectory is generated, the value $-\Delta E_{in}$ gives rise to a different local mode trajectory;

(b) the same local mode can be obtained either from an initial condition A or S (with two appropriate values of E_{in});

(c) the transition modes are obtained only with an initial condition S if $K < 0$ (or A if $K > 0$). These modes are influenced from the initial phase relation like normal modes are, but they have different trajectories when the sign of initial energy difference ΔE_{in} is changed, like local modes do.

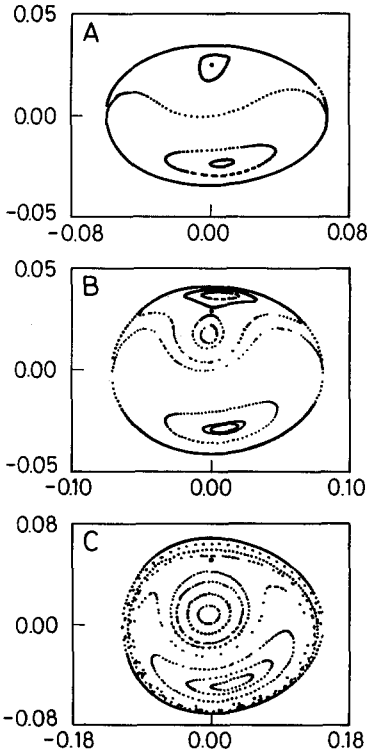

Fig. 5A–C. Poincaré surfaces of section for two Morse oscillators coupled both potentially and kinetically, at three different values for the total energy E_T. $K = +0.1$ mdyne/Å; $G = -(1/36)$ a.m.u.$^{-1}$. Both oscillators start from the vibrational equilibrium. Ordinate axes are p_2 (units: a.m.u. A femtosec^{-1}). Abscissas are Δl_2 (units: Å). **A** $E_T = 500\ \text{cm}^{-1}$. *lh:* antisymmetric normal modes. *hh:* symmetric normal modes. In both cases the curves are ordered from inside with $\Delta E_{in} = 0, 250\ \text{cm}^{-1}$. Separating curve at $\Delta E_{in} = 500\ \text{cm}^{-1}$. **B** $E_T = 700\ \text{cm}^{-1}$. *lh:* antisymmetric normal modes, from inside: 0, 100, 350 cm^{-1}. *hh:* symmetric normal modes and transition modes. *Central dot:* $\Delta E_{in} = 0$, symmetric normal mode. *Inner couples of circles:* $\Delta E_{in} = \pm 350, \pm 100\ \text{cm}^{-1}$ (from inside), transition modes; *bilobed curve:* $\Delta E_{in} = 690\ \text{cm}^{-1}$, symmetric normal mode. **C** $E_T = 2000$ cm. *lh:* antisymmetric normal modes, from inside $\Delta E_{in} = 0, 500, 1000, 1500\ \text{cm}^{-1}$, *A. hh:* local modes. *Couples of curves* from inside: $\Delta E_{in} = \pm 2000, \pm 1500, \pm 1000, \pm 500, \pm 100\ \text{cm}^{-1}$, *S*

3. Perturbative treatment

In the literature the problem of two coupled nonlinear oscillators has also been analyzed by classical perturbation theory [11–13]. In this section we compare our numerical experiments on the CH_2 molecular fragment with analytical models already used by these authors.

Given a non-integrable Hamiltonian $H(\Delta l_1, \ldots, \Delta l_n, p_i, \ldots, p_n)$, like in Eq. (1), one can always express it as a function of action and angle variables ϕ_i, I_i of an integrable Hamiltonian H_0 so that:

$$H = \sum_i \{H_0(I_i)\} + \varepsilon V(I_1, \ldots, I_n, \phi_i, \ldots, \phi_n) \quad (5)$$

For the system discussed above the most used choice for H_0 is that of uncoupled

nonlinear Morse oscillators [12, 13] (first term in Eq. (1)); the coupling terms of Eqs. (1) and (4) have usually been treated as the angle dependent term εV of Eq. (5). ϕ_i and I_i thus are the angle and action variables of two uncoupled Morse oscillators, whose expression can be found for example in [12]. The two oscillators have frequencies ω_i which are action dependent:

$$\omega_i(I_i) = \omega_i^h(1 - I_i/I_i^d) \quad I_i^d = \sqrt{2D_i m/a_i^2} \tag{6}$$

where the constants ω_i^h, D_i, m, and a_i have been introduced in the previous section. I_i are the actions at the dissociation energy.

$\sum_i H_0(I_i^d)$ alone originates a pure local mode regime, since the two oscillators are completely independent: the oscillators cannot exchange energy or influence each other to get a preferential phase relation. Only the term $V(I_1, I_2, \phi_1, \phi_2)$ in Eq. (5) can give rise to normal modes. A standard procedure [29] is to expand, in the coupling terms of the original Hamiltonians of Eq. (1) or (4), actions and angles in Fourier series obtaining sums of terms containing $\cos(n_1\phi_1 - n_2\phi_2)$ over pairs (n_1, n_2) of relative prime positive integers and all their multiples or harmonics [12]. When $n_1\omega_1 - n_2\omega_2 = 0$ for a given pair (n_1, n_2) a resonance is met, referred to as the $n_1 : n_2$ resonance. Usually each resonance is studied decoupled from the others. This is done, foir example, to study overlapping resonances [26, 29, 30] which become important at high energy in the study of statistical energy distribution. In the case presented here, where the two CH oscillators (identical for the numerical experiments above) are at relatively low energies, only the 1 : 1 resonance is important. This resonance has already been indicated as responsible for the presence of normal modes at low energies [12, 13]. After Fourier expansion and decoupling of the $n_1 = n_2 = 1$ resonance, the resulting total Hamiltonian (in wavenumber units) adapted from [12] to our case is:

$$\begin{aligned}\frac{H}{hc} = {} & 2\chi J_2(J_1 - J_2) + \frac{\varepsilon K}{4\pi^2 mc^2\chi}\left\{\tfrac{1}{2}\ln\left[\frac{2(I_d - J_2)^2}{2I_d^2 - I_d J_2}\right]\ln\left[\frac{2(I_d - J_1 + J_2)^2}{2I_d^2 - I_d J_1 + I_d J_2}\right]\right. \\ & \left. + \sum_{k=1}^{\infty}\left(\frac{J_2}{2I_d - J_2}\frac{J_1 - J_2}{2I_d - J_1 + J_2}\right)^{k/2}\frac{1}{k^2}\cos k\theta_2\right\} \\ & + \varepsilon\frac{G_{12} m\omega_h^2}{\chi}\left(1 - \frac{J_2}{I_d}\right)\left(1 - \frac{J_1 - J_2}{I_d}\right)\frac{1 - \alpha_1\alpha_2\cos\theta_2}{1 - 2\alpha_1\alpha_2\cos\theta_2 + (\alpha_1\alpha_2)^2}\end{aligned} \tag{7}$$

where equivalence of the two oscillators has been assumed, namely $\chi_1 = \chi_2 = \chi$, $\omega_1^h = \omega_2^h = \omega_h$ and $I_1^d = I_2^d = I_d$, and where:

$$\alpha_i = \sqrt{I_i/(2I_d - I_i)}$$

Equation (7) has been written with the canonical transformation mentioned in [12], namely:

$$J_1 = I_1 + I_2 \qquad \theta_1 = \phi_1$$

$$J_2 = I_1 \qquad \theta_2 = \phi_1 - \phi_2$$

and further terms depending on J_1 only have been neglected, since J_1 is an integral of motion and ϕ_1 its cyclic coordinate.

Herein we have not yet reduced the Hamiltonian to an expansion around the resonant periodic orbit, as it is usually done to study overlapping resonances

[26, 30]. This procedure has also been employed to obtain an analytical expression of the resonance width, that is the extent of normal modes [11–13] and consequently the critical value of I_i, above which local modes are present [12]. In our treatment, instead, the coefficients of the angle dependent terms $\cos(k\theta_2)$ are not evaluated at the resonance (that is at $J_2 = J_1/2$): the εV part depends both on J_2 and θ_2. By use of a graphic algorithm developed at the Department of Physics at the University of Milano, we have plotted the phase space curves in the plane (J_2, θ_2) of the Hamiltonian of Eq. (7) for various values of H/hc corresponding to all the cases examined by numerical integration on the exact Hamiltonian in the previous section. The sum on the harmonics of the resonance angle θ_2 that appears in the potential has been truncated at $k = 2$, since it converges rapidly enough.

In Fig. 6 we present the phase space portrait at three different values for J_1 with $K = \pm 0.1$ mdyne/Å and $G_{12} = 0$. In Fig. 7 three cases are shown for the system with $K = +0.1$ mdyne/Å and G_{12} defined as in Eq. (4). In abscissa the angle θ_2 represents the phase relation of the two oscillators. For the ordinate $J_2 - (J_1/2)$ (that is $(I_1 - I_2)/2$) is proportional to the instantaneous energy difference ΔE (ΔE_{in} considered in the previous paragraph corresponds to $J_2 - (J_1/2)$ at $\theta_2(t = 0)$). $\Delta E_{\max}$ can label univocally the phase space curves independently of the value of θ_2 at time $t = 0$. The three regimes in Figs. 6 and7, for the three increasing values of J_1, correspond satisfactorily to the three regimes found by numerical integration. These figures must be compared with Figs. 2 and 5.

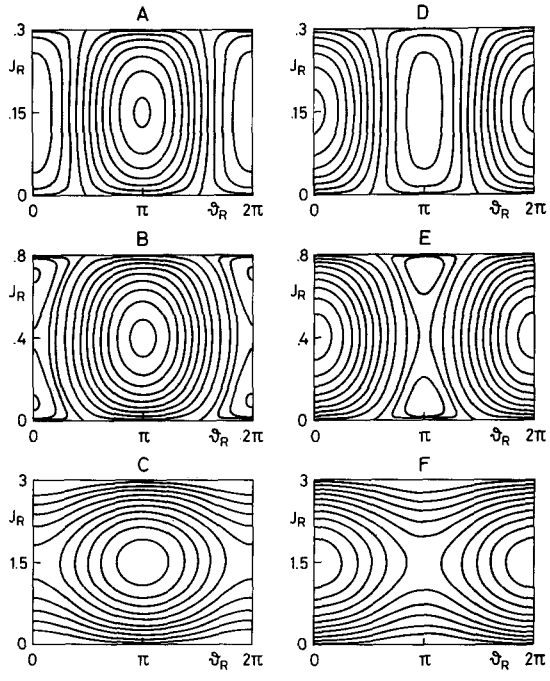

Fig. 6A–F. Trajectories in the phase space of the resonant angle and its conjugated action associated to the system of two Morse oscillators coupled linearly through a potential term. One curve differs from the next for a constant difference in the values attributed to H/hc defined in Eq. (7) in the text ($G_{12} = 0$). (**A–C**) $K = -0.1$ mdyne/Å; (**D–F**) $K = +0.1$ mdyne/Å. (**A,D**) Total action $J_1 = 0.3$; (**B,E**) $J_1 = 1.0$; (**C,F**) $J_1 = 3$ (see text)

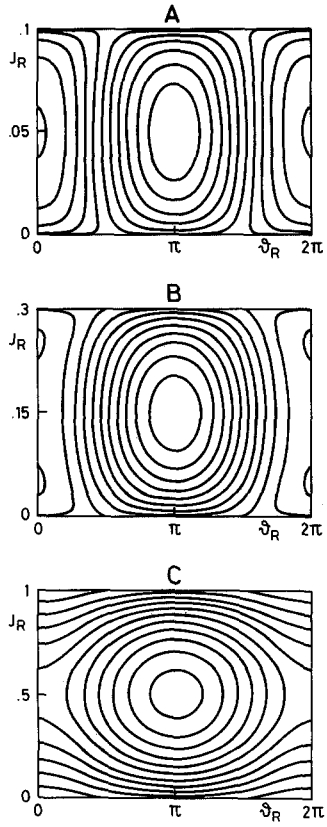

Fig. 7A–C. Trajectory in the phase space of the resonant angle and its conjugated action associated to the system of two Morse oscillators coupled linearly both potentially and kinetically. One curve differs from the next for a constant difference in the values attributed to H/hc defined in Eq. (7) in the text. $K = +0.1$ mdyne/Å, $G_{12} = -(1/36)$ a.m.u.$^{-1}$. **(A)** Total action $J_1 = 0.1$: **(B)** $J_1 = 0.3$; **(C)** $J_1 = 1$

At low values for J_1 (Figs. 6A, 6D, and 7A) all curves are closed, that is to say along each curve, θ_2 cannot assume all values and this corresponds to what we have called above phase locking. Furthermore, all curves are centered either at $\theta_2 = 0$ or at $\theta_2 = \pi$, and at $J_2 = J_1/2$ in both cases, so that both the symmetric and the antisymmetric modes are stable. Since each closed curve is symmetric with respect to $J_1/2$, energy is exchanged between the two oscillators in the same way as in Fig. 1A. Thus all modes are normal modes (the two oscillators have equal mean energies and are phase locked).

At intermediate values for J_1, as can be seen in Figs. 6B and 7B, one can notice that for negative K (or effective K) the symmetric mode is a saddle point and there are two new centers, one corresponding to positive ΔE ($J_2 > J_1/2$) and one to negative ΔE ($J_2 < J_1/2$) exactly as it is observed in the PSS of Figs. 2B and 5B. The same phenomenon is observed for the antisymmetric mode when K is positive (Fig. 6E). The curves are closed, thus the modes are phase locked, but, around the new centers, J_2 is either always higher than $J_1/2$ or always lower, so that the mean energies of the two oscillators are not equal anymore. Thus the presence of these new centers corresponds to the transition modes found previously. In the first and second regimes all the curves in the PSS are confined to two noncommunicating regions, corresponding to two separate intervals for θ_2; this can be related to the fact that the plots of T vs. $\Delta E_{\max}$ in Figs. 3A and 3B give different curves when starting from initial condition $S(\theta_2 = 0)$ or

A ($\theta_2 = \pi$). In the second regime, with the two new centers (in Fig. 6B for example at $\theta_2 = 0$) the corresponding plot of T vs. $\Delta E_{\max}$ of Fig. 3B for initial condition S is a cusp, indicating a transition between two families of curves. Indeed going along the $\theta_2 = 0$ axis, from $(J_1/2)$ to J_1 (ΔE_{in} from 0 to E_T) one first meets the two intersections of the small circles with the θ_2 axis and thus covers twice the left side of the cusp of Fig. 3B (as indicated by the two different symbols for the data). Further increasing J_2, one meets the large curves (reminiscent of the first regime) encircling both the central saddle point and the new centers, and this can be put in correspondence with the right side of the cusp of Fig. 3B, that is normal modes.

In the third regime, at higher J_1, the centers assigned to transition modes disappear and the phase space portrait is like that of a pendulum (Figs. 6C, 6F and 7C): the closed curves around the stable fixed point correspond to normal modes and the open curves (no phase locking), correspond to local modes. This picture, already well known in the literature [11–13] is related to the cusps of Fig. 3C, which is typical of a pendulum too, as already noted. Furthermore, in the case with $K = -0.1$ mdyne/Å for example, it is clear that the complete cusp can be obtained at $\theta_2\,(t=0) = \pi$, that is where the resonance width is maximum (this corresponds to the circles in the Figure); at $\theta_2\,(t=0) = 0$ instead, only the local mode side of the cusp can be obtained (squares in the Figure). The value $\Delta E*$ at the cusp is proportional to value for $I_1 - I_2$ of the separatrix between open lines and closed curves.

It can be noted that in the last regime we can approximate Eq. (7) by taking $V(J_2, \theta_2) = V(J_2 = J_1/2, \theta_2)$ as already done in [12] and [13]. In this way the perturbative part depends only on θ_2 and can be treated analytically more easily. Consequently, the relative phase θ_2 satisfies equation:

$$\dot{\theta}_2 = \tfrac{1}{2}(\omega_1 - \omega_2) = (\omega_h^2/2D)(I_2 - I_1) \propto -\Delta E \tag{8}$$

Transition modes cannot be described in this approximation: indeed if ΔE is always negative (for example when E_2 is always higher than E_1), Eq. (8) implies that θ_2 increases indefinitely and thus no phase locking can occur, opposite to what found in Fig. 4.

Instead, the exact time behavior of the resonant angle-action couple (θ_2, J_2) can be obtained from Hamilton's equations associated with the Hamiltonian equation (7), which are (ignoring the kinetic contribution):

$$\dot{J}_2 = -\frac{1}{hc}\frac{\partial H}{\partial \theta_2} = \sum_{k=1}^{\infty}\left(\frac{J_2}{2I_d - J_2}\frac{J_1 - J_2}{2I_d - J_1 + J_2}\right)^{k/2}\frac{1}{k}\sin k\theta_2 \tag{9'}$$

$$\begin{aligned}\dot{\theta}_2 = \frac{1}{hc}\frac{\partial H}{\partial J_2} &= 2\chi(J_1 - 2J_2) \\ &+ \frac{\varepsilon K}{8\pi^2 mc^2\chi}\frac{(-3I_d + J_2)}{(I_d - J_2)(2I_d - J_2)}\ln\left\{\frac{2(I_d - J_1 + J_2)^2}{I_d(2I_d - J_1 + J_2)}\right\} \\ &+ \frac{\varepsilon K}{8\pi^2 mc^2\chi}\frac{(3I_d - J_1 + J_2)}{(I_d - J_1 + J_2)(2I_d - J_1 + J_2)}\ln\left\{\frac{2(I_d - J_2)^2}{I_d(2I_d - J_2)}\right\} \\ &+ \frac{\varepsilon K}{8\pi^2 mc^2\chi}\sum_{k=1}^{\infty}\left[\frac{J_2(J_1 - J_2)}{(2I_d - J_2)(2I_d - J_1 + J_2)}\right]^{k/2-1} \\ &\times \frac{2I_d(J_1 - 2J_2)(2I_d - J_1)}{(2I_d - J_1 + J_2)^2(2I_d - J_2)^2}\frac{1}{k}\cos k\theta_2\end{aligned} \tag{9''}$$

The system of Eq. (9) admits fixed points ($\dot{J}_2 = 0, \dot{\theta}_2 = 0$) at $\theta_2 = 0$, π and $J_2 = (J_1/2)$. Inserting $J_2 = (J_1/2)$ into the three terms of Eq. (9″), they vanish identically. These fixed points have already been found in the literature and correspond to either symmetric or antisymmetric normal modes. However, at either $\theta_2 = 0$ for $K < 0$ or $\theta_2 = \pi$ for $k > 0$ another couple of filxed points can be found. In order to prove this, let us take for simplicity only the first term in the cosine series of Eq. (9″) and assume that the action at dissociation I_d (which is equal to 25 in the case studied in Sect. 2 of the present paper) is much greater than J_1 and J_2. One can then prove straightforwardly that the following couple of fixed points symmetrically disposed about $(J_1/2)$ arises on the lines $\theta_2 = 0$ or π:

$$J_2 = J_1/2 \pm A \tag{10′}$$

where:

$$\left[\left(\frac{J_1}{2}\right)^2 - A^2\right]^{1/2} = -\left(\frac{K}{8\pi^2 mc^2 \chi}\right)\frac{1}{4\chi I_d}\cos\theta_2 \tag{10″}$$

Equation (10″) makes sense under the following circumstances:

(a) if $K > 0$ at $\theta_2 = \pi$; if $K < 0$ at $\theta_2 = 0$;

(b)
$$J_1 \geqslant \frac{(K/4\pi^2 mc^2)}{2\chi\omega^h} \cong \frac{\Delta}{2\chi} \tag{11}$$

where $\Delta = |\omega_+ - \omega_-|$, ω_+ and ω_- being the harmonic frequencies of the symmetric and antisymmetric normal modes. The condition expressed by Eq. (11) has been obtained by substituting $I_d = \omega^h/2\chi$ [13]. Under those circumstances:

$$A = \left[\left(\frac{J_1}{2}\right)^2 - \frac{(K/4\pi^2 mc^2)^2}{(2\chi)^4 (2I_d)^2}\right]^{1/2}$$

The latter couple of fixed points corresponds to transition modes: they are found to appear close to symmetric or antisymmetric normal modes according to the sign of K, as already proved in the numerical experiments presented in Sect. 2.

The validity of the threshold for transition modes predicted by Eq. (11) was also tested numerically. In Table 1 we show the values of the total energy E_T for which transition modes appear, according to the numerical integration of the classical equations of motions associated with the Hamiltonian of Eq. (1). Since, in a first approximation $E_T \propto J_1$, we can state that Eq. (11) is perfectly valid. In particular for the case $\omega^h = 3000\ \text{cm}^{-1}$, $\chi = 60\ \text{cm}^{-1}$ and $K = -0.1$ mdyne/Å one obtains $\Delta = 56.5\ \text{cm}^{-1}$ and thus the threshold predicted by Eq. (11) is $J_1 = 0.478$. The approximate value for $J_1 = E_T/\omega^h$ calculated from the entries of Table 1 is 0.521, which nicely compares with the predicted value. In Table 1 we have also reported the value $E_{\max}$ for E_T for which most of the transition modes have disappeared; also $E_{\max}$ seems to be proportional to Δ/χ, but we have not yet the analytical explanation for it.

Finally, exactly the same value for J_1 is found by studying the change in stability of the fixed point at $\theta_2 = 0$ (π) and $J_2 = J_1/2$, from the eigenvalues of

Table 1. Values of the total energy E_T for the appearance (E_{min}) and disappearence (E_{max}) of transition modes calculated by numerical integration of Eq. (1) for a few values of χ and K ($\omega^h = 3000\ cm^{-1}$)

χ (cm^{-1})	K (mdyne/Å)	E_{min} [a] (cm^{-1})	E_{max} [b] (cm^{-1})
50	−0.1	1951	10200
55	−0.1	1800	9300
60	−0.1	1630	8600
65	−0.1	1500	7700
70	−0.1	1395	7100
60	−0.05	800	4500
60	−0.07	1150	5890
60	−0.15	2460	11900
50	−0.2	3458	14700

[a] E_{min} is the value of E_T for which the symmetric fixed point changes from stable to unstable

[b] E_{max} is the value of E_T for which the curve for $\Delta E_{in} = 95\%\ E_T$ is still inside the curve for $\Delta E_{in} = E_T$ (see text)

the Hessian matrix $\boldsymbol{T}$:

$$\det(\boldsymbol{T} - \lambda \boldsymbol{I}) = \det \begin{bmatrix} \dfrac{\partial^2 H/hc}{\partial\theta_2\,\partial J_2} - \lambda & \dfrac{\partial^2 H/hc}{\partial J_2^2} \\ -\dfrac{\partial^2 H/hc}{\partial\theta_2^2} & -\dfrac{\partial^2 H/hc}{\partial\theta_2\,\partial J_2} - \lambda \end{bmatrix} = \lambda^2 + \frac{\partial^2 H/hc}{\partial J_2^2}\frac{\partial^2 H/hc}{\partial\theta_2^2}$$

Making the simplifying assumptions on the actions discussed above, one can prove that at $J_2 = (J_1/2)$:

$$\lambda^2 = -\frac{2K}{4\pi^2 mc^2}\left[\left(\frac{J_2}{I_d}\right)\cos\theta_2 + \frac{K}{8\pi^2 mc^2\omega^{h2}}(\cos\theta_2)^2\right]$$

Indeed for $K < 0$ at $\theta_2 = 0$, λ goes from imaginary (stable fixed point) to real (unstable fixed point) for the same value of J_1, predicted in Eq. (11). For $K \geqslant 0$ this happens for $\theta_2 = \pi$.

4. Conclusions

In this paper the classical mechanics of the system of two linearly coupled equivalent Morse oscillators has been investigated at low to moderate total energy by two methods, namely by numerical integration and by a perturbative treatment in which the zeroth-order approximation has been based on local modes. By the first method we found that at low total energy E_T only normal modes are present, at high E_T values normal and local modes are coexisting, while in between a third kind of mode is predicted (the transition modes) showing some characteristic features of both normal and local modes. The

same kind of picture is obtained by the perturbative treatment that was proposed in the literature and that we have examined in full detail at variable total action.

It may seem that the conclusions just drawn are dependent on the form of the Hamiltonian of Eq. (1) or on the values of the parameters ω_i^h, χ_i, and K. As far as the latter parameter is concerned we tried values ranging from $|K| = 0.01$ mdyne/Å to $|K| = 0.2$ mdyne/Å, and values for $\chi_1 = \chi_2$ from 50 to 70 cm^{-1}: we found that the same picture holds except that different thresholds for the different regimes are calculated numerically and predicted via perturbative treatment. As far as the form of the Hamiltonian is concerned, the insertion of the kinetic interaction term G_{12} does not alter the picture. Besides, from preliminary investigations, we think that this picture holds also if the interaction potential term is nonlinear like, e.g., that proposed in [19].

In conclusion, it looks like that the existence of transition modes is related to the evolution of a stable fixed point to an unstable one. The mechanism implied by this evolution is *first* a loss of energy correlation between the two bond modes and *later* a loss of phase correlation. Only when these two independent processes are completed, the transition from normal modes to local modes is complete. We then think that the existence of transition modes is fairly universal and could be spectroscopically checked. In order to find the spectroscopic "signature" of transition modes, the following characteristic should be kept in mind: from our calculations it appears that the intermediate energy region comprising transition modes is broader the larger the interaction constant is with respect to intrinsic bond anharmonicity (namely its width is proportional to Δ/χ). Further work is in progress in this field in our laboratories, together with the development of a classical perturbative treatment based on normal modes.

Acknowledgements. We would like to thank Professor A. Giorgilli from Dipartimento di Fisica, Università di Milano, for illuminating discussions. We thank Professor N. Terzi from the same Department and we also thank Istituto di Chimica delle Macromolecole, C.N.R., Milano for use of their computer time. This work was done in part under the auspices of an international collaboration program between University of Palermo and C.N.R.S., France.

References

1. Hayward RJ, Henry BR (1975) J Mol Spectrosc 57:221; Henry BR (1981) in: Durig JR (ed) Vibrational spectra and structure vol X, Chap 4, Elsevier, NY
2. Swofford RL, Long ME, Albrecht AC (1976) J Chem Phys 65:179
3. Bray RG, Berry MJ (1979) J Chem Phys, 71:4909; Burberry MS, Albrecht AC (1979) J Chem Phys 71:4631
4. Henry BR, Tarr AW, Mortensen OS, Murphy WF, Compton AC (1983) J Chem Phys 79:2583
5. Abbate S, Longhi G, Ricard L, Bertucci C, Rosini C, Salvadori P, Moscowitz A (1989) J Am Chem Soc 111:836
6. Mills IM, Robiette AG (1985) Mol Phys 56:743
7. (a) Lehmann KK (1983) J Chem Phys 79:1098; (b) Lehmann KK (1986) J Chem Phys 84:6524
8. Della Valle RG (1988) Mol Phys 63:611
9. Xiao L, Kellman ME (1989) J Chem Phys 90:6086 and references therein
10. Lawton RT, Child MS (1979) Mol Phys 37:1799
11. Child MS, Halonen L (1985) Adv Chem Phys LVII:1
12. Jaffé C, Brumer P (1980) J Chem Phys 73:5646

13. Sibert EL III, Reinhardt WP, Hynes JT (1982) J Chem Phys 77:3583
14. Li Z, Xiao L, Kellman ME (1990) J Chem Phys 92:2251
15. Sibert EL III, Hynes JT, Reinhardt WP (1983) J Phys Chem 87:2032
16. Dübal HR, Quack M (1984) J Chem Phys 81:3779
17. Reddy KV, Heller DF, Berry MJ (1982) J Chem Phys 76:2814
18. Mc Coy S, Lehmann KK (1989) Spectrochim Acta 45A:47; Scherer J, Klemperer W, Lehmann KK (1983) J Chem Phys 78:2817
19. Halonen L (1989) J Phys Chem 93:3386
20. Sibert EL III (1989) J Chem Phys 90:2672; Gray SK, Davis MJ (1989) J Chem Phys 90:5420
21. Iachello F, Levine RD (1982) J Chem Phys 77:3046;
van Roosmalen OS, Iachello F, Levine RD, Diepetrink AEL (1983) J Chem Phys 79:2515
22. Hutchinson J (1988) Adv Chem Phys LXIII:637
23. Wilson EB Jr, Decius JC, Cross PC (1955) Molecular vibrations. McGraw-Hill, NY
24. Thiele E, Wilson DJ (1961) J Chem Phys 35:1256
25. Lawton RT, Child MS (1981) Mol Phys 44:709
26. Chirikov BV (1979) Phys Rep 52:269
27. Zagano C (1987) Tesi di Laurea in Fisica, Università di Milano
28. Snyder RG, Schachtschneider JH (1963) Spectrochim Acta 19A:85
29. Brumer P (1980) Adv Chem Phys XLVII:201
30. Oxtoby DW, Rice SA (1976) J Chem Phys 65:1676